Journal of Molecular Structure 1272 (2023) 134113

Contents lists available at ScienceDirect

Journal of Molecular Structure

journal homepage: www.elsevier.com/locate/molstr

Tautomerization of diazene<=>hydrazine *via* single proton tautomerization, spectral, XRD/HSA-interactions, optical and DFT/TD-DFT of new hydrazine ligand

Assia Mili[a,b], Souheyla Chetioui[a,c], Amel Djedouani[d,e,**], Jean-Pierre Djukic[f], Abeer AlObaid[g], Abdelkader Zarrouk[h], Ismail Warad[j,*]

[a] Unité de Recherche de Chimie de l'Environnement et Moléculaire Structurale, (CHEMS), Faculté des Sciences Exactes, Département de Chimie, Université des Frères Mentouri, Constantine 1, Constantine 25000, Algérie
[b] Ecole Nationale Supérieure de Biotechnologie Taoufik Khaznadar (ENSB), ville universitaire Ali Mendjli, Constantine 3, Algerie
[c] Faculté de Technologie, Université Mohamed Boudiaf M'sila, Algérie
[d] Laboratoire de Physicochimie Analytique et Cristallochimie des Matériaux Organométalliques et Biomoléculaires, Université Constantine 1, 25000, Algérie
[e] Ecole Normale Supérieure de Constantine Assia-Djebbar, Université Constantine 3, 25000, Algérie
[f] Laboratoire de Chimie et Systémique Organométallique (LCSOM), Université de Strasbourg, UMR 7177, F-67070 Strasbourg Cedex, France
[g] Department of Chemistry, College of Science, King Saud University, P.O. Box 2455, Riyadh 11451, Saudi Arabia
[h] Laboratory of Materials, Nanotechnology and Environment, Mohammed V University in Rabat, Faculty of Sciences, Av. Ibn Battuta, PO B.P. 1014, Rabat, Morocco
[j] Department of Chemistry, Science College, An-Najah National University, Nablus P.O. Box 7, Palestine

ARTICLE INFO

Article history:
Received 16 February 2022
Revised 5 September 2022
Accepted 6 September 2022
Available online 9 September 2022

Keywords:
Hydrazine
XRD
DFT
HSA
Tautomerization
Spectral analysis

ABSTRACT

A novel methyl (Z)-2-(2-(2-oxonaphthalen-1(2H)-ylidene)hydrazineyl)benzoate isomer ligand has been prepared instead of (*E*)-methyl 2-((2-hydroxynaphthalen-1-yl)diazenyl)benzoate isomer in very good yield. The tautomerization of diazene to hydrazine was computed via DFT; the single proton tautomerization S(6) process was confirmed by XRD. Moreover, the XRD-crystal measurements supported the hydrazine form as the preferred kinetic isomer; the structure of the desired ligand was also examined by IR, UV–vis., Carbon, Hydrogen and Nitrogen elemental analysis (CHN-EA), and NMR. Hirshfeld surface analysis (HSA) computation was performed to support the lattice interactions resulting by X-ray diffraction (XRD) measurement. Furthermore, the time-dependent density functional theory (TD-DFT) and B3LYP/IR computation were used to support the UV–visible as well as FT-IR experimental results.

1. Introduction

Azo-ligands are essential in the field of dyes and advanced materials [1] as they possess strong chromophores properties and have long been used as pigments [2–18]. It has numerous applications such as the coloring of diverse materials, the dyeing of textile fibers, coloring polymers and plastics, medicinal-biological activities, and advanced applications in organic syntheses [2–5]. Lately, Azo-ligands have attracted attention in coordination chemistry due to their various industrial applications [6–9]. They have also many applications in the field of optical data storage and nonlinear optics [10–13]. The optical properties of such material depend on the spectroscopic properties and their crystallographic arrangements [14,15]. In general, 1-phenylazo-2-naphthol can coexist in azo and hydrazone tautomer forms [16–18]. Hydrazone form have an ionic intra-molecular hydrogen bond (N^+–H· · ·O^-) and their N^+–H bond lengths are longer than the standard interatomic [19].

The tautomerization azo/hydrazone was discovered in 1884 by Zincke and his collaborators [20]. Their study was carried out on an orange dye that was obtained by coupling the chloride of benzenediazonium with 1-naphthol and condensation by the phenylhydrazine with 1,4-naphtoquinone, and the products obtained were the azo and the hydrazone dye. This discovery has stimulated the researchers to invest in the phenomenon of tautomerization; which is extremely interesting for commercial azo-dye in addition tautomers have different properties [21].

* Corresponding author.
** Corresponding author at: Laboratoire de Physicochimie Analytique et Cristallochimie des Matériaux Organométalliques et Biomoléculaires, Université Constantine 1, 25000, Algérie.
E-mail addresses: djedouani_amel@yahoo.fr (A. Djedouani), warad@najah.edu (I. Warad).

https://doi.org/10.1016/j.molstruc.2022.134113
0022-2860/

In our group we are interested in the synthesis of several types of polychelate ligands and their transition metal complexes for their application as catalysts and medicinal compounds [22–29]. Following our previous work we describe the synthesis and crystal structure of a new azo compound namely: (E)-methyl 2-((2-hydroxynaphthalen-1-yl)diazenyl)benzoate and study its structural isomerization [21,29-31].

Herein, the Diazene<=>hydrazine tautomerization process of methyl (Z)-2-(2-(2-oxonaphthalen-1(2H)-ylidene)hydrazineyl) benzoate to methyl (Z)-2-(2-(2-oxonaphthalen-1(2H)-ylidene)-hydra-zineyl)benzoate in MeOH was figured out by NMR and XRD. The process was computed by DFT and the final product was confirmed by XRD-crystal analysis. Hydrazine isomer including CHN-elemental analysis, FT-IR, NMR and UV–vis spectroscopy. The experimental bond vibrations and the absorption results have been compared via B3LYP/lR and TD-DFT respectively.

2. Experimental

2.1. Measurements and materials

2-benzoate aniline and naphtol were used as received. Elemental analyses were carried out by the service of analyses, physical measurements and optical spectroscopy (C.N.R.S-University of Strasbourg, France). NMR spectra were recorded in DMSO-d_6 on a Brücker Avence DPX-type spectrophotometer, 300 MHz, TMS as internal reference, chemical shift in ppm. Infrared spectra were recorded with a Fourier transform infrared spectrometer (ALPHA) FTIR from the brand BRUKER, controlled by Opus 6.5 software and fitted with an Attenuated Total Reflectance (ATR) accessory in diamond crystal. UV spectra were recorded on an Agilent UV–vis spectrophotometer 8453 (spectroscopy system) with G1120A multicell transport and a computer with ChemStation (Visible Ultra Violet 1120 A).

2.2. Computational and XRD-analysis details

Gaussian 09W 32 bit software served for all DFT operations in gaseous state at DFT/B3LYP method and 6-311++G(d,p) as basis set [32,33]. The Hirshfeld surface analysis was carried out using Crystal Explorer 3.1 [34].

A single crystal was carefully selected mounted on a Bruker Apex II [31], CCD area detector diffractometer with a graphite mono-chromated Mo-Kα radiation source (0.71073 Å), intensities were collected at 293 (2)°K. Structure was solved by direct methods with SIR2002 [35,36], to locate all the non-H atoms which were refined anisotropically with SHELXL97 [37] using full-matrix least squares on F2 procedure within the WinGX [34] suite of software used to prepare the material for publication [38]. Absorption corrections were performed with the MULABS program [39]. The H atoms were included in calculated positions and treated as riding atoms. The Mercury for Windows program were used for generating figures of structures [40]. The main crystal parameters are presented in Table 1. Angles and bond distances of are listed in **S1** and **S2**.

2.3. Synthesis

The (*E*)-methyl 2-((2-hydroxynaphthalen-1-yl)diazenyl)benzoate ligand was synthesized through the diazotization of 2-benzoat aniline followed by a coupling reaction with β-naphthol according to the established procedure [41]. The methyl (Z)-2-(2-(2-oxonaphthalen-1(2H)-ylidene)hydrazineyl)benzoate was prepared via tautomerization of (*E*)-methyl 2-((2-hydroxynaphthalen-1-yl)diazenyl)benzoate in methanol. The obtained orange solid, was washed with ice water, dried and recrystallized from THF–H_2O (1:1 v/v) solution, to afford orange crystals, Yield: 88%. Anal. Calc. for $C_{18}H_{14}N_2O_3$, C, 68.58%, N, 9.15%, and H, 4.61%, found C, 68.12%, N, 8.92%, and H, 4.64%. ^{1}H NMR (DMSO-d_6, 300MHz), δ ppm: 1.6 (s, 3H, O-*CH3*); 5.5 (d, H_β); 6.1 (d, H_α) in the naphtol group respectively; the aromatic protons appear as multiple signal in the 7.25-6 range. ^{13}C NMR (DMSO–d_6, 300 MHz): 56.1, 122.30 - 135.02, 143.22, 166, 179.

Table 1
Crystallographic data and structure refinement details of the ligand.

$C_{18}H_{14}N_2O_3$	Empirical formula
2108225	CCDC
306.31	Formula weight, g/mol
$P2_1$ /c, Monoclinic	Space group, Crystal system
0.04× 0.03× 0.02	Dimensions du monocristal (mm^3)
full-matrixleast-squareson *F*2	Refinement method
3.7983(5), 23.5756(19), 15.8272(18) 94.041(10)	a (Å), b (Å), c (Å), β(°)
1413.8(3), 4, 640	V(Å^3), Z, F(000)
293(2)	Temperature/K
3.369° - 67.825°	θ Range for data collection (°)
Cu Kα (λ= 1.54186)	Radiation
1.439	d_{calcd} (g/cm^{-3})
-4≤ h ≤4, -27≤ k ≤27, -18≤ l ≤18	Range/indices (h, k, l)
10,426	Ref Nmb of reflections measured
2466	independent reflections
2056	Reflections with I > 2σ(I)
213	Number of parameters
0.816	Absorption coefficient (mm^{-1})
1.086	Goodness-of-fit (GOF)
0.1508	wR(F2)
0.0580	Rint

3. Results and discussion

3.1. Synthesis

The (*E*)-methyl 2-((2-hydroxynaphthalen-1-yl)diazenyl)benzoate (HL) was synthesized via the diazotization then tautomerization of 2-benzoate aniline followed by a coupling reaction with β-naphthol in a high yield, as describe in Scheme 1. The synthesized azo-dye is air stable, soluble in polar solvents and insoluble in non-polar, moreover, the desired ligand was characterized by NMR, IR, CHN-EA and UV–vis. spectroscopy, and single crystal X-ray diffraction analysis. The hydrazine isomer methyl (Z)-2-(2-(2-oxonaphthalen-1(2H)-ylidene)hydrazineyl)benzoate was found to be favored over the diazenyl isomer methyl (E)-2-((2-hydroxynaphthalen-1-yl)diazenyl)benzoate since the first one structure has been confirmed via XRD structure for the first time. The DFT simulation was performed to explain the single proton intra-migration transfer process.

3.2. XRD-crystal and DFT-optimization analysis

It can be seen that the (*E*)-methyl 2-((2-hydroxynaphthalen-1-yl)diazenyl)benzoate diazene isomer has undergone a fundamental tautomerization in its structure where the hydrogen atom has moved from the hydroxyl group to form the hydrazine methyl (Z)-2-(2-(2-oxonaphthalen-1(2H)-ylidene)hydrazineyl)benzoate *via* tautomerization in methanol. The final product hydrazine isomer was crystallized in the monoclinic system in $P2_1/c$ space group, the unit cell contains four molecules, scheme of the molecule structure, with the atom numbering, is shown in (Fig. 1a). The final 3D-structure computed by the DFT as shown in the (Fig. 1b) is consistent with the experimental crystallographic measurements results. In both methods, the molecule is the Z-isomer with quite planar and the most important deviation is observed for the car-

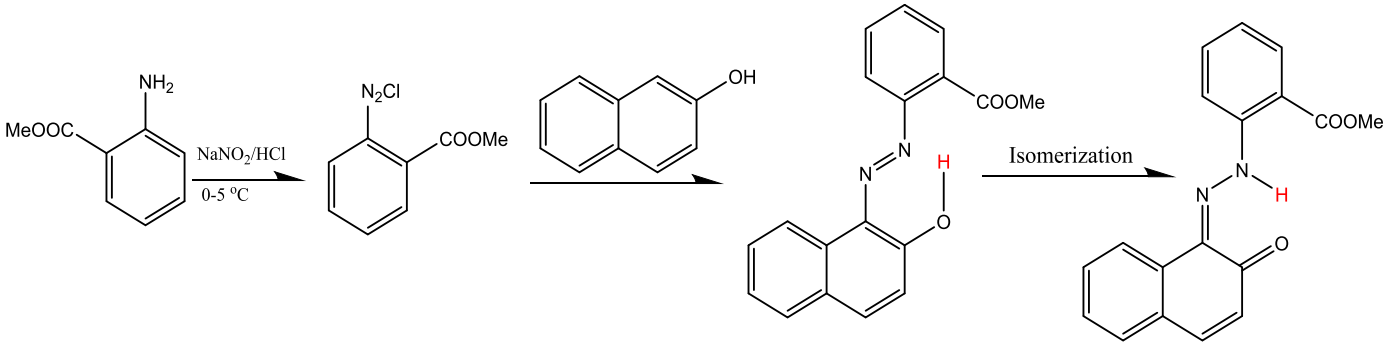

Scheme 1. Synthesis of desired ligand.

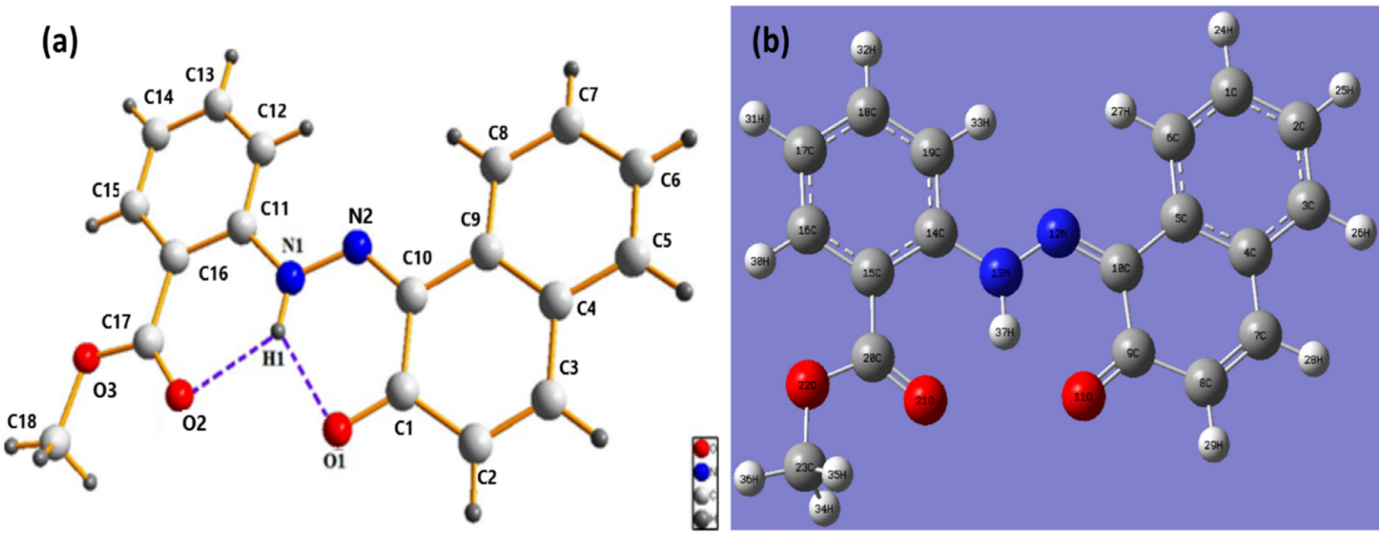

Fig. 1. (a) ORTEP with intra-H-bonds, and (b) DFT-optimization structures.

bon C18:0,141 Å, the rings of benzene and naphtol are in the (*E*) position with the -N=N- bond, the same configuration is observed for same compounds [42,43]. Moreover, all the angles and bond lengths of benzene and naphthol were consistent with previous studies [44–46].

3.3. XRD-packing and Hirshfeld surface analysis

The molecule adopts zwitterionic form (i.e. the proton from the hydroxyl in the naphthol group is transferred to the azo-group), the two groups are linked by an intramolecular N1—H1…O1 hydrogen bond, enclosing an S6 ring motif [47,48]. The same hydrogen atom participates in a second intramolecular hydrogen bond N1—H1…O2 enclosing another S6 ring motif (Fig. 2). The dihedral angle between the two rings is 1.97°. C1–$O1_{Hydroxy}$ bond length [1.238(2) Å] is intermediate between double and single oxygen to carbon bond lengths (1.362 Å, 1.222 Å) [49]. The distances O1-C1/C1-C10/C10-N2 and N2-N1 exhibit intermediate distances between a single and a double bond because of resonance [50,51]. In the crystal molecules deploy in zig zag and are aligned head to tail along the *b* axis, in columns parallel to [001] plan giving rise to an infinite chain directed by two interactions C18—H18B···O1 and C18-H18A…O2 (Table 2), generate $R^2_2(10)$ loops (Fig. 2). In addition, π…π interaction is observed, involving naphthalene ring systems and benzene ring of adjacent molecules along a axis, the centroid–centroid distance equal 3.798(7) Å, helps to stabilize the crystal structure.

Table 2
Distances [**D—H···A, D—H, H···A, D···A**] (Å) and angles [**D—H···A**] (°) of H-bonds for (HL).

Ligand				
D—H···A	D—H	H···A	D···A	D—H···A
N1—H1···O1	0.881 (5)	1.897 (19)	2.597 (3)	135.15 (18)
N1—H1···O2	0.881 (5)	2.045 (16)	2.674 (3)	127.48 (2)
C18—H18A···O2	0.960 (4)	2.570 (12)	3.484 (2)	159.30 (4)
C18—H18B···O1	0.960 (4)	2.689 (14)	3.166 (2)	107.58 (5)

3.4. Diazene<=>hydrazine isomerization via single proton intra-migration

As the final product obtained by the XRD-diffraction showed that, the final structure of the desired ligand is methyl (Z)-2-(2-(2-oxonaphthalen-1(2H)-ylidene)hydrazineyl)benzoate instead of (*E*)-methyl 2-((2-hydroxynaphthalen-1-yl)diazenyl)benzoate the expected isomer. For this reason, it was necessary to conduct theoretical calculations to figure out which structure is favored (more stable) and simulate how structural isomerization was performed. The methanol phase Diazene<=>hydrazine proton transfer was examined via DFT/B3LYP-simulation, and the transition state (TS) was stimulated by the $TS_{(Bernyl)}$ method [6,19].

The gaseous state-DFT-computational of H transfer process suggested that the proton OH of phenol group moved toward the N=N functional group via intramolecular hydrogen bond proton

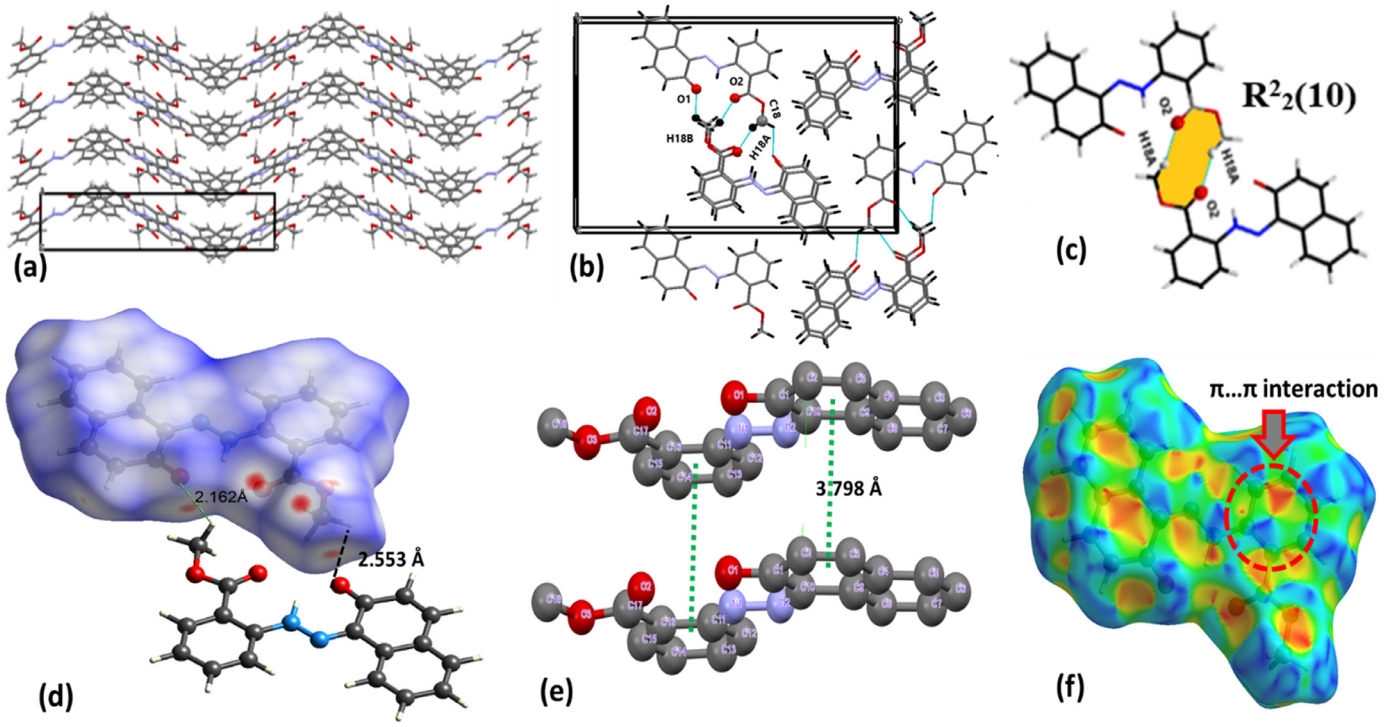

Fig. 2. (a) Cell packing along the axis c, (b) view of part of the crystal structure along the *a* axis of the title compound. C–H…O interactions, (c) comprising cage-like aggregates containing $R^2_2(10)$ rings, (d) HSA d_{norm} including H…O H-bonds, (e) π to π interactions, and (f) shape index showing stack bonds.

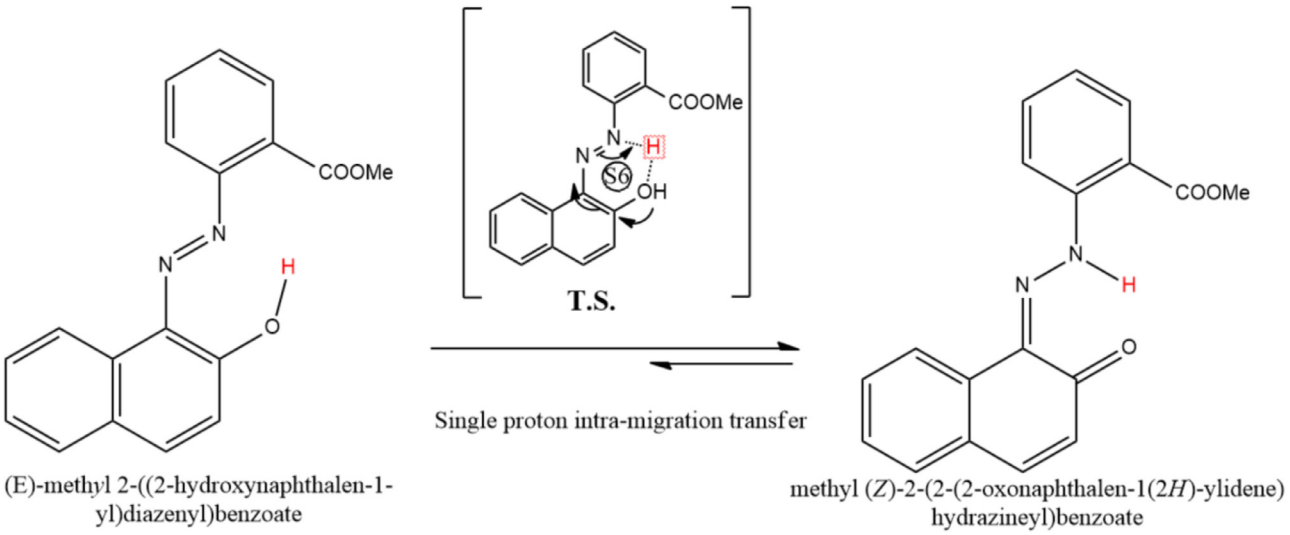

Scheme 2. Prototropic diazene (-OH)<=>hydrazine (-NH) isomerization.

migration constructing S6 O–H…N transition state as illustrated in Scheme 2. The [O^-…H-N^+] interaction can be suggested with prototropic process includes shorted N–H bond 0.838 Å and longer O-H distance 1.798 Å. Hammond postulate the T.S properties to be with hydrazine more than diazene and E_{TS} = 138.9 kJ/mol, as illustrated in (Fig. 3). However, DFT calculation reflected the hydrazine form as a more stable than diazene isomer since it is less with −24.2 kJ/mol, such energy amount is not significant, therefore, the possibility for such isomerization increased since MeOH as polar solvents with high solvation energy was used here experimentally as well as theoretically. Moreover, such result is harmonic with what XRD-achievement.

3.5. ^{1}H- and ^{13}C-NMR analysis

In the ^{1}H NMR (S3a), most of the protons are observed in aromatic area as multiple signals in the 7.25–6.0 range [48], the two doublet signals appeared at 6.1 and 5.5 ppm (d, J = 7.8 Hz) assigned to H_1 and H_2 hydrogens in the naphtol group respectively, peak at 1.6 ppm attributed to methoxyl group [52,53]. Moreover, the absence of H-N peak as high chemical shift is attributed to D-exchanged process between the DMSO-d6 solvent and the desired compound.

In the ^{13}C NMR (S3b), the signal resonated at 56.1 ppm is assigned to the methoxyl carbon [54,55]. The appearance of a col-

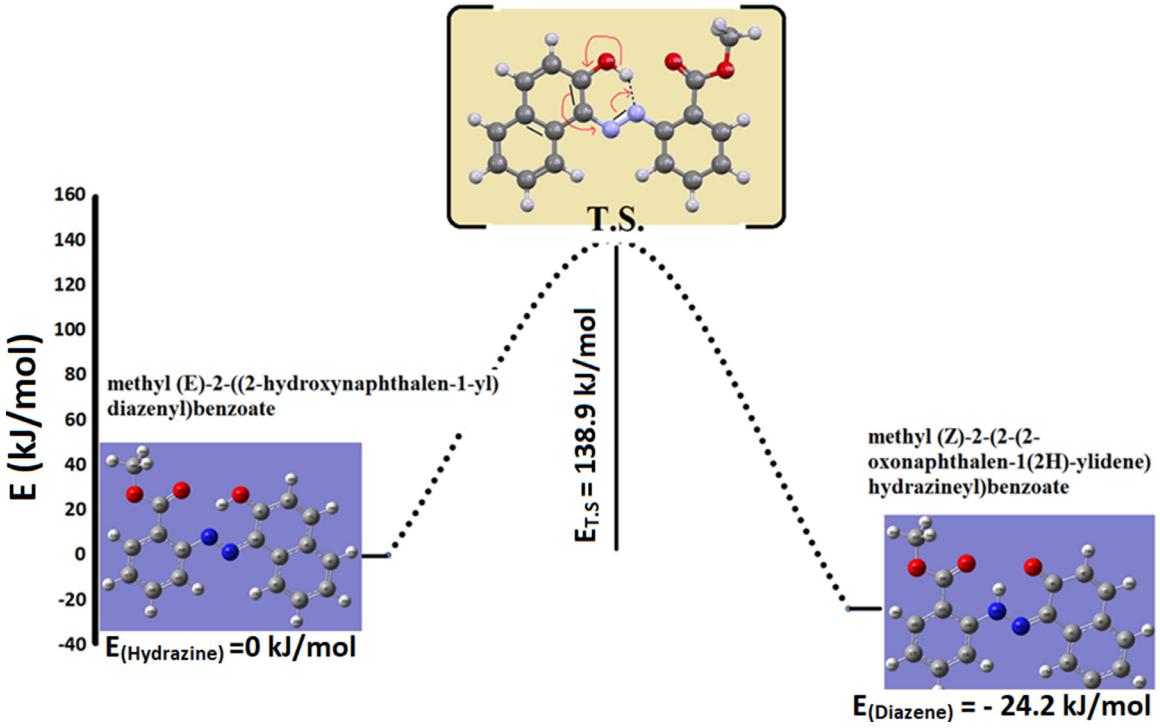

Fig. 3. GS-DFT diazene<=>hydrazine isomerization energy profiles.

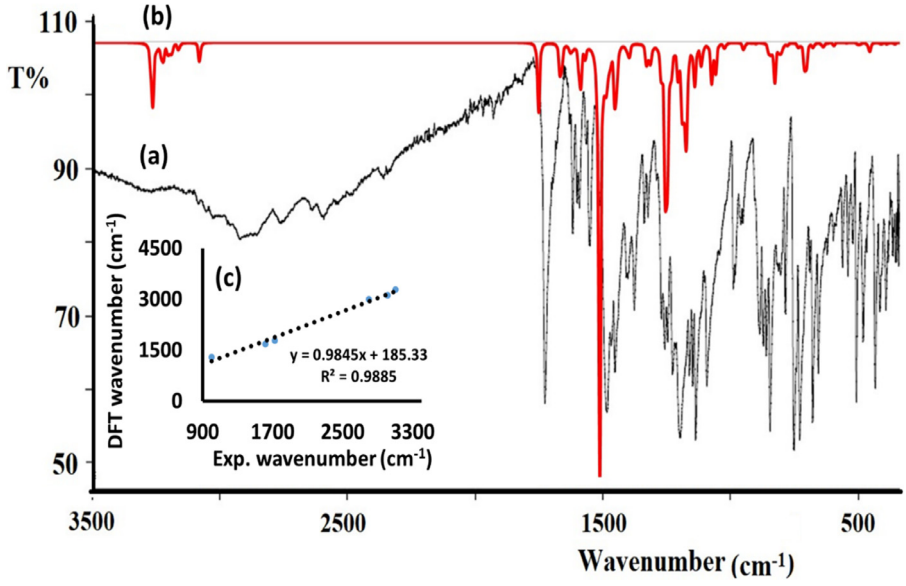

Fig. 4. (a) Exp. FT-IR, (b) B3LYP-IR, and (c) B3LYP/FT-IR graphical correlation.

lection of signals in the region (122.30–135.02) ppm are assigned to aryl carbons and C=N signal resonated at 143.22 ppm. Interestingly, two peaks in carbonyl region were detected, one is attributed to ester C=O at 179 ppm and the other one at 166 ppm can be attributed to the hydrazine C=O, therefore, ^{13}C NMR supported the presence of ketone C=O due to hydrazine isomer formation that is consistent with result observed by the XRD.

3.6. FT-IR analysis

The νC–H of phenyls peaks are observed at ~3050 cm^{-1} and νC-H of MeO at 2980–2885 cm^{-1}. The N–H stretching bands was not observed in the range of 3300 cm^{-1} due to the N-H…O=C intra hydrogen bond formation [56]. The νC=O absorption band of ester is detected at 1700 cm^{-1}, meanwhile, the νC=O absorption band of ketone at 1620 cm^{-1} and the IR spectra showed bands around 1555 cm^{-1} which can be assigned to the νC=N [57–59]. The bands appearing between 1400 and 1600 cm^{-1} can be assigned to the stretching modes of the benzene rings [59]. Furthermore (-OCH$_3$) stretching vibrations are observed around 1000 cm^{-1} [60]. To understand better the stretching vibrations behavior of the desired ligand, IR/DFT-theoretical calculations were carried out under DFT/B3LYP/611++G(d,p) level as illustrated in (Fig. 4a). All the signs of functional groups that appeared by IR/DFT are in agreement (Fig. 4b) with the experimental IR, moreover, a high graphical correlation (0.9885) was recorded as seen in (Fig. 4c).

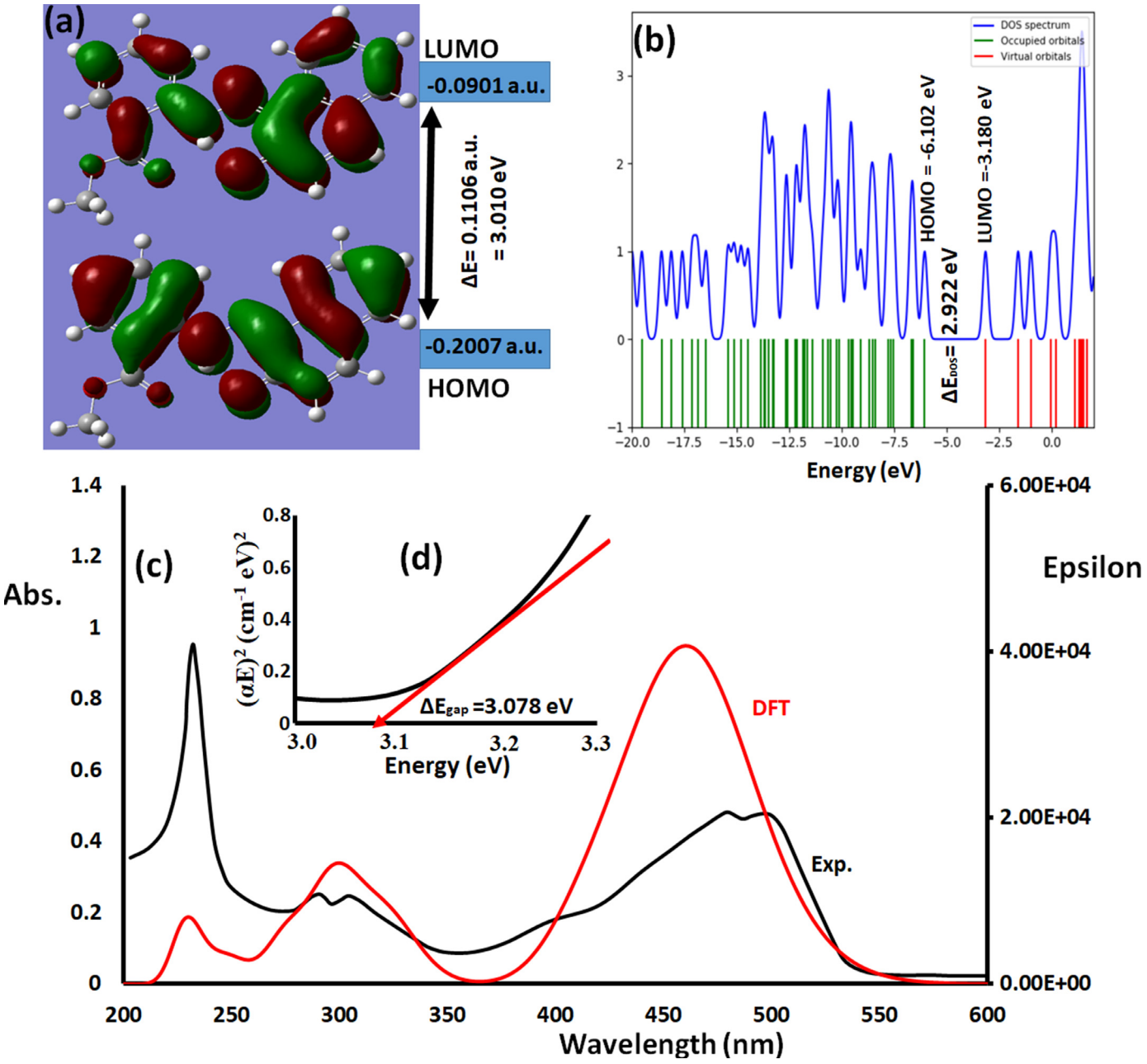

Fig. 5. (a) HOMO/LUMO, (b) DOS, and (c) UV–vis./TD-DFT/B3LYP and (d) Tuac's optical diagram in MeOH.

3.7. UV–vis. and TD-DFT analysis

The experiment electronic behavior, computation HOMO/LUMO, DOS and absorption TD-DFT/B3LYP spectra of the desired ligand was recorded in methanol solution at room temperature [56–66]. HOMO/LUMO and DOS energy gabs showed very similar values 3.010 eV (Fig. 5a) and 2.922 eV (Fig. 5b) respectively, therefore, in the event that the electron moved from HOMO to LUMO, the value of the wavelength energy needed to exit it will go with 412 nm in the case of $\Delta E_{HOMO/LUMO}$ and 424 nm in the case of ΔE_{DOS}. In the experimental UV-vis. spectrum, λ_{max} at 282 nm can be assigned to the $\pi \rightarrow \pi^*$ transitions in the aromatic rings [61]. The λ_{max} at 285 and 303 nm assigned to the $\pi \rightarrow \pi^*$ transition which involve the π electrons of the azo group [62]. Another band with two peaks at 478 and 494 nm is attributed to hydrazine structure (Fig. 5c). The TD-DFT/B3LYP was performed in the MeOH solvent; in order compare the result with the UV–vis. absorption under identical conditions as illustrated in (Fig. 5c). The TD-DFT/B3LYP [63–65] calculations reflected the presence of several transitions, the energies, excitation wavelengths, oscillator strengths (f) and percent composition in forms of LUMO and HOMO dissolved MeOH solution are illustrated in Table 3 (only the first ten transitions with f>0.03 were recorded). The mean three peaks at 232 nm attributed to H-9=>LUMO (27%), and H-3=>L+1(68%), 302 nm attributed to H-5=>LUMO (71%), HOMO =>L+1(23%) and H-1=>L+1(3%), and 467 nm attributed to HOMO =>LUMO (100%) as be seen in Table 4 and Fig. 5c. A very small (1–10 nm) absorption shift between experimental and calculated λ_{max} values were noted [56–69]. The bandgap energy (E_g) of the desired ligand was calculated from Tauc's equations [70] using Eq. (1). The experimental value of

Table 3
TD-DFT/B3LYP data in MeOH.

No.	E (cm^{-1})	λ(nm)	Osc. St.(f)	Major contribs	Minor contribs
1	21530.9	476.8	0.515	HOMO->LUMO(100%)	
2	23650.6	422.8	0.166	H-1->LUMO(97%)	
3	30831.4	324.3	0.0367	H-5->LUMO(17%), H-3->LUMO(34%), HOMO->L+1(45%)	
4	31097.5	321.6	0.0696	H-3->LUMO(62%), HOMO->L+1(29%)	H-5->LUMO(6%)
5	33519.6	304.1	0.1756	H-5->LUMO(71%), HOMO->L+1(23%)	H-1->L+1(3%)
6	36169.1	276.5	0.0836	HOMO->L+2(93%)	H-1->L+ (2%)
7	39622.8	252.4	0.0189	H-7->LUMO(87%)	H-1->L+3(3%), H->L+3(3%)
8	40764.9	245.3	0.0303	H-1->L+2(71%), HOMO->L+3(24%)	
9	43166.8	233.9	0.0416	H-9->LUMO(27%), H-3->L+1(68%)	
10	43845.9	228.1	0.0703	H-9->LUMO(57%), H-3->L+1(25%), HOMO->L+4(10%)	

the indirect E_g was found to be 3.078 eV as seen in Fig. 5d which is very close to E_{DOS} and $E_{HOMO/LUMO}$ theoretical values.

$$ahv = A(hv - E_g)^n \quad (1)$$

4. Conclusion

The novel hydrazine methyl (Z)-2-(2-(2-oxonaphthalen-1(2H)-ylidene)hydrazineyl)benzoate ligand isomer, was directly prepared *via* tautomerization of (*E*)-methyl 2-((2-hydroxynaphthalen-1-yl)diazenyl)benzoate in MeOH solvent with 88% yield. The kinetic favored hydrazine isomer has been confirmed by XRD-crystal measurements; moreover, IR, UV–vis., CHN, and NMR were used to support the physicochemical properties of hydrazine ligand form. The single proton [O–H to N–H] intra-migration [diazene<=>hydrazine] tautomerization has been computed *via* the DFT in order to prove the superiority of hydrazine isomer over diazene one. The HSA computation interactions reflected the presence of several [H…O and H…N] intra-hydrogen bonds supporting the XRD-packing results. Moreover, the B3LYP/IR and TD-DFT computation results were agreed to a very high degree with the experimental FT-IR and UV–vis results respectively.

Declaration of Competing Interest

No potential conflict of interest was reported by the authors.

Data Availability

No data was used for the research described in the article.

Acknowledgments

The auteurs acknowledge the Algerian Ministry of Higher Education and Scientific Research, the Algerian Directorate for Scientific Research and Technological Development, and Constantine 1 University for financial support. Mme Corine Bailly from University of Strasbourg, France, is thanked for the collecting data.

Funding

The authors extend their appreciation to the Researchers Supporting Project number (RSP-2021/381), King Saud University, Riyadh, Saudi Arabia.

References

[1] K. Hunger, Industrial Dyes, Chemistry, Properties and Applications, Wiley-VCH, Weinheim, 2003, pp. 20–35. edited by K. Hunger.
[2] S.C. Catino, & R.E. Farris, Azo dyes, in: Concise Encyclopedia of Chemical Technology, John Wiley and Sons, New York, 1985, pp. 142–144. edited by M. Grayson.
[3] H. Zollinger, Colour Chemistry: Synthesis, Properties and Applications of Organic Dyes and Pigments, 3rd rev. ed., Wiley-VCH, Weinheim, 2003 edited by H. Zollinger.
[4] H.S. Bahatti, S. Seshadri, Synthesis and fastness properties of styryl and azo disperse dyes derived from 6-nitro substituted 3-aryl-2-methyl-4(3H)-quinazolinone, Color. Technol. 120 (2004) 151–155.
[5] K. Taniike, T. Matsumoto, T. Sato, Y. Ozaki, K. Nakashima, K. Iriyama, Spectroscopic Studies on Phase Transitions in Langmuir−Blodgett Films of an Azobenzene-Containing Long-Chain Fatty Acid: Dependence of Phase Transitions on the Number of Monolayers and Transition Cycles among H-, J-, and J'-Aggregates in Multilayer Films, J. Phys. Chem. 100 (1996) 15508–15516.
[6] S. Chetioui, A. Djedouani, Z. Fellahi, J-Pierre Djukic, Christian G. Bochet, A. Zarrouk, I. Warad, Diazene<=>hydrazine tautomerization in MeOH, single proton intra-migration, XRD/HSA-interactions, spectral, optical and DFT/TD-DFT of new hydrazine, J. Mol. Struct. 229 (2021) 129604–129610.
[7] S. Chetioui, D.A. Rouag, J-P. Djukic, C.G. Bochet, R. Touzani, A.Crochet C.Bailly, K.M. Fromm, Crystal structures of a copper (II) and the isotypic nickel(II) and palladium(II) complexes of the ligand (E)-1-[(2, 4, 6-tribromophenyl) diazenyl] naphthalen-2-ol, Acta Cryst E72 (2016) 1093–1098.
[8] A. Mili, S. Chetioui, D.A. Rouag, J-P. Djukic, C. Bailly, Chlorido {(E)-1-[(2-methoxyphenyl) diazenyl] naphthalen-2-olato} palladium (II), IUCrData 1 (2016) X160691.
[9] S. Chetioui, N. Hamdouni, D.A. Rouag, S. Bouaoud, H. Merazig, Crystal structure of bis {1-[(E)-(2-methoxyphenyl) diazenyl] naphthalen-2-olato-κ3O, N2, O′} copper (II) containing an unknown solvate, Acta cryst E71 (2015) m207–m208.
[10] A. Fadda, H.A. Etmen, F.A. Amer, M. Barghout, K.S.J. Mohammed, Azo disperse dyes for synthetic fibres. I: 2-Methyl-and 2-phenylquinazolone derivatives, J. Chem. Technol. Biotechnol. 61 (1994) 343–349.
[11] H. Bach, K. Anderle, Th. Fuhrmann, J.H. Wendorff, Biphoton-induced refractive index change in 4-amino-4 '-nitroazobenzene/polycarbonate, J. Phys. Chem. 100 (1996) 4135–4140.
[12] R.J.H. Clark, R.E. Hester, Spectroscopy of New Materials: Advances in Spectroscopy, John Wiley and Sons, New York, 1993 edited by R. J. H. Clark & R. E. Hester.
[13] S. Wang, S. Shen, H. Xu, Synthesis, spectroscopic and thermal properties of a series of azo metal chelate dyes, Dyes Pigments 44 (2000) 195–198.
[14] N. Biswas, S. Umapathy, Structures, vibrational frequencies, and normal modes of substituted azo dyes: infrared, Raman, and density functional calculations, J. Phys. Chem. A. 104 (2000) 2734–2745.
[15] I. Willner, S. Rubin, Angew. Control of the structure and functions of biomaterials by light, Chem. Int. Ed. Engl. 35 (1996) 367–385.
[16] S. Chetioui, I. Boudraa, S. Bouacida, A. Bouchoul, S. Bouaoud, E)-1-[(2, 4, 6-Tribromophenyl) diazenyl] naphthalen-2-ol, Acta Cryst E69 (2013) o1250–o1251.
[17] S. Chetioui, M. Boutebdja, M. Boudraa, R. Touzani, H. Merazig, E)-1-[2-(3, 4-Dimethylphenyl) diazen-2-ium-1-yl] naphthalen-2-olate, IUCrData 2 (2017) X170259.
[18] S. Chetioui, M. Chikhi, M.A. Benaouida, H. Bougueria, A. Bouchoul, Diazene<=>hydrazine tautomerization in MeOH, single proton intra-migration, XRD/HSA-interactions, spectral, optical and DFT/TD-DFT of new hydrazine, Int. J. Pharm. Biomed. Sci. 4 (2013) 113–118.
[19] A. Guerraoui, A. Djedouani, E. Jeanneau, A. Boumaza, A. Alsalme, A. Zarrouk, K.S.M. Salih, I. Warad, Crystal structure and spectral of new hydrazine-pyran–dione derivative: DFT enol↔hydrazone tautomerization via zwitterionic intermediate, hirshfeld analysis and optical activity studies, J. Mol. Struct. 1220 (2020) 128728–128738.
[20] T. Zincke, H. Binderwald, Ueber Phenylhydrazinderivate des α-und β-Naphtochinons. Identität des α-Derivats mit dem Azoderivat des α-Naphtols, Chem. Ber. 17 (1884) 3026–3036.
[21] S-T. Lin, L-H. Lin, Y-C. Lin, M-F. Ding, Substituent Effect on the Tautomerization of 1-Arylazonaphthalen-2-ols by Mass Spectrometric Analysis, J. Chin. Chem. Soc. 62 (2015) 257–262.
[22] S. Chetioui, N. Hamdouni, C.G. Bochet, J-P Djukic, C. Bailly, Crystal structure of bis-{[mu]-1-[(E)-(3-meth-oxy-phen-yl)diazen-yl]naphthalen-2-olato-[kappa]3N2,O:O}bis-({1-[(E)-(3-meth-oxy-phen-yl)diazen-yl]naphthalen-2-olato-[kappa]2N2,O}copper(II)), Acta Cryst E71 (2015) m211–m212.
[23] S. Chetioui, B. Zouchoune, H. Merazig, S.–E Bouaoud.D. A.Rouag, J–P Djukic, Synthesis, spectroscopic characterization, crystal structure and theoretical investigation of two azo-palladium (II) complexes derived from substituted (1-phenylazo)-2-naphtol, Transt. Met. Chem. 46 (2021) 91–101.
[24] S. Chetioui, H. Bougueria, O. Brihi, N.Bouroumane M.Boutebdja, H. Meraziga, R. Touzani, Diazene<=>hydrazine tautomerization in MeOH, single proton in-

tra-migration, XRD/HSA-interactions, spectral, optical and DFT/TD-DFT of new hydrazine, Acta Cryst E76 (2020) 382–386.
[25] I. Warad, A.F. Eftaiha, M.A. Al-Nuri, A.I. Husein, M. Assal, A. Abu-Obaid, N. Al-Zaqri, T. Ben Hadda, B. Hammouti, Metal ions as antitumor complexes-Review, J. Mater. Environ. Sci. 4 (2013) 542–557.
[26] I. Warad, A.A. Khan, M. Azam, S.I. Al-Resayes, S.F. Haddad, Design and structural studies of diimine/CdX2 (X= Cl, I) complexes based on 2, 2-dimethyl-1, 3-diaminopropane ligand, J. Mol. Struct. 1062 (2014) 167–173.
[27] F. Abu Saleemh, S. Musameh, A. Sawafta, P. Brandao, C.J. Tavares, S. Ferdov, A. Barakat, A. Al Ali, M. Al-Noaimi, I. Warad, Diethylenetriamine/diamines/copper(II) complexes [Cu(dien)(NN)]Br2: Synthesis, solvatochromism, thermal, electrochemistry, single crystal, Hirshfeld surface analysis and antibacterial activity, Arab. J. Chem. 10 (2017) 845–854.
[28] M. Rbaa, M. Ouakki, M. Galai, A. Berisha, B. Lakhrissi, C. Jama, I. Warad, A. Zarrouk, Simple preparation and characterization of novel 8-Hydroxyquinoline derivatives as effective acid corrosion inhibitor for mild steel: Experimental and theoretical studies, Coll. Surf. A 602 (2020) 125094–125118.
[29] V. Deneva, A. Lyčka, S. Hristova, A. Crochet, K.M. Fromm, L. Antonov, 7-OH quinoline Schiff bases: are they the long awaited tautomeric bistable switches, Dyes and Pigments 165 (2019) 57–163.
[30] K. Hamidian, M. Irandoust, E. Rafiee, M. Joshaghani, Synthesis, characterization, and tautomeric properties of some azo-azomethine compounds, Z. Naturforsch 67b (2012) 159–164.
[31] A. Liudmil, Tautomerism in Azo and Azomethyne Dyes: When and If Theory Meets Experiment, Molecules 24 (2019) 2252–2265.
[32] M.J. Frisch, G.W. Trucks, H.B. Schlegel, G.E. Scuseria, et al., Gaussian 09W, Gaussian Inc., Wallingford CT, 2009.
[33] R. Dennington, T. Keith, J. Millam, Gauss View Version 5, Semichem Inc., Shawnee Mission, 2009.
[34] S.K. Wolff, D.J. Grimwood, J.J. McKinnon, M.J. Turner, D. Jayatilaka, M.A. Spackman, Crystal Explorer 3.0, University of Western Australia, Perth, 2012.
[35] Bruker APEX2 and SAINT, Bruker AXS Inc., Madison, Wisconsin, USA., 2007.
[36] M.C. Burla, R. Caliandro, M. Camalli, B. Carrozzini, G.L. Cascarano, L. DeCaro, C Giacovazzo, G. Polidori, R. Spagna, SIR2004: an improved tool for crystal structure determination and refinement, J. Appl. Crystallogr. 38 (2005) 381–390.
[37] G.M. Sheldrick, A short history of SHELX, Acta Crystallogr., Sect A64 (2008) 112–122.
[38] L.J. Farrugia, WinGX and ORTEP for Windows: an update, J. Appl. Cryst. 45 (2012) 849–854.
[39] A.L. Spek, Structure validation in chemical crystallography, Acta Cryst D65 (2009) 148–155.
[40] C.F. Macrae, I.J. Bruno, J.A. Chisholm, P.R. Edgington, P. McCabe, E. Pidcock, L. Rodriguez-Monge, R. Taylor, J. van de Streek, P.A. Wood, Mercury CSD 2.0–new features for the visualization and investigation of crystal structures, J. Appl. Cryst. 41 (2008) 466–470.
[41] M. Wang, K. Funabiki, M. Matsui, Synthesis and properties of bis (hetaryl) azo dyes, Dyes Pigments 57 (2003) 77–86.
[42] A. Mili, A. Benosmane, S. Chetioui, A. Bouchoul, XRD Data analysis of 1-(2, 5-dimethoxyphenylazo)-2-naphtol, J. Chem. Pharm. Res. 5 (2013) 12–18.
[43] M.A. Benaouida, S. Chetioui, S.E. Bouaoud, 1-(4-Hydroxyphenyl)-2-(2-oxidonaphthalen-1-yl) diazen-1-ium methanol hemisolvate, Acta cryst E69 (2013) o867–o868.
[44] H. Bougueria, M.A.Bensegueni S.Chetioui, J.P. Djukicd, N. Benarousa, Crystal structure and Hirshfeld surface analysis of 1-[(E)-2-(5-chloro-2-hydroxyphenyl) hydrazin-1-ylidene] naphthalen-2 (1H)-one, Acta Cryst E77 (2021) 672–676.
[45] H. Bougueria, S. Chetioui, I. Boudraa, A. Bouchoul, S. Bouaoud, E)-1-(2-Phenyldiazen-2-ium-1-yl) naphthalen-2-olate, Acta cryst E69 (2013) o1335–o1336.
[46] H. Bougueria, S. Chetioui, A. Mili, S. Bouaoud, H. Merazig, E)-1-(4-Fluorophenyl)-2-(2-oxidonaphthalen-1-yl) diazen-1-ium, IUCrData (2017) X170039.
[47] A. Benosmane, M.A. Benaouida, A. Mili, A. Bouchoul, H. Merazig, Crystal structure of 1-[(Z)-2-phenylhydrazin-1-ylidene] naphthalen-2 (1H)-one, Acta cryst E71 (2015) o303–o304.
[48] A. Benosmane, A. Mili, H. Bouguerria, A. Bouchoul, E)-1-(3-Chlorophen-yl)-2-(2-oxidonaphthalen-1-yl)diazen-1-ium, Acta Cryst E69 (2013) o1021–o1022.
[49] F.H. Allen, O. Kennard, D.G. Watson, L. Brammer, A.G. Orpen, R. Taylor, Tables of bond lengths determined by X-ray and neutron diffraction. Part 1. Bond lengths in organic compounds, J. Chem. Soc., Perkin Trans.II (1987) S1–S19.
[50] A. Djedouani, B. Anak, S. Tabti, F. Cleymand, M. François, S. Fleutot, Crystal structure and DFT study of the zwitterionic form of 3-{(E)-1-[(4-ethoxyphenyl) iminiumyl] ethyl}-6-methyl-2-oxo-2H-pyran-4-olate, Acta Cryst E74 (2018) 172–175.
[51] S. Chetioui, I. Boudraa, S. Bouacida, A. Bouchoul, S. Bouaoud, 1-[(E)-2-(2-Hydroxy-5-methylphenyl) diazen-2-ium-1-yl] naphthalen-2-olate, Acta Cryst E69 (2013) o1322–o1323.
[52] A. Bhowmick, M. Islam, R. Bhowmick, M. Sarkar, A. Shibly, E. Hossain, Synthesis and structure determination of some schiff base metal complexes with investigating antibacterial activity, Am. J. Chem. 9 (1) (2019) 21–25.
[53] A.E. Şabik, M. Karabörk, G. Ceyhan, M. Tümer, M. Dığrak, Polydentate Schiff base ligands and their La (III) complexes: Synthesis, characterization, antibacterial, thermal, and electrochemical properties, Int. J. Inorg. Chem. 2012 (2012) 1–12.
[54] H. Ünvera, M Yıldızb, B. Dülger, Ö. Özgend, E. Kendid, T.N. Durlua, Spectroscopic studies, antimicrobial activities and crystal structures of N-(2-hydroxy-3-methoxybenzalidene) 1-aminonaphthalene, J. Mol. Struct. 737 (2005) 159–164.
[55] C. Şenol, Z. Hayvali, H. Dal, T. Hökelek, Syntheses, characterizations and structures of NO donor Schiff base ligands and nickel(II) and copper(II) complexes, J. Mol. Struct. 997 (2011) 53–59.
[56] S. Özkar, D. Ülkü, L.T. Yildirim, N. Biricik, B. Gümgüm, Crystal and molecular structure of bis (acetylacetone) ethylenediimine: intramolecular ionic hydrogen bonding in solid state, J. Mol. Struct. 688 (2004) 207–211.
[57] M. Gavranic, B. Kaitner, E. Mestrovis, p-electron delocalization in N-aryl Schiff bases of 2-hydroxy-1-naphthaldehyde: the crystal structures of planar N-(a–naphthyl) and N-(b-naphthyl)-2-oxy, Chem. Crystallogr. 26 (1996) 23–28.
[58] H.H. Freedman, Intramolecular H-bonds. I. A spectroscopic study of the hydrogen bond between hydroxyl and nitrogen, J. Am. Chem. Soc. 83 (1961) 2900–2905.
[59] Y. Yang, S. Pan, X. Hou, J. Guo, F. Li, J. Han, J. Guo, D. Jia, Syntheses, structures and properties of three nonmetal borates with salicylic acid and organic amines, Inorg. Chim. Acta. 365 (2011) 20–24.
[60] A. Fatoni, P.L. Hariani, A.Lesbani Hermansyah, synthesis and characterization of Schiff base 4, 4-diaminodiphenyl ether vanillin possessed of free primary amine, IOP Conf, J. Phys. Conf. Series 1095 (2018) 1–9.
[61] M.R. Hasan, M.A. Hossain, Md.A. Salam, M.N. Uddin, Nickel complexes of Schiff bases derived from mono/diketone with anthranilic acid: Synthesis, characterization and microbial evaluation, J. Taibah. Univ. Sci. 10 (2016) 766–773.
[62] N. Al-Zaqri, T. Pooventhiran, A. Alsalme, I. Warad, M. John, R. Thomas, Synthesis, structural, biocomputational modeling and antifungal activity of novel armed pyrazoles, J. Mol. Liq. 318 (2020) 114082–114092.
[63] B.M. Wong, T.H. Hsieh, Optoelectronic and excitonic properties of oligoacenes: substantial improvements from range-separated time-dependent density functional theory, J. Chem. Theory Comput. 6 (2010) 3704–3712.
[64] A.E. Raeber, B.M. Wong, The importance of short-and long-range exchange on various excited state properties of DNA monomers, stacked complexes, and Watson–Crick Pairs, J. Chem. Theory Comput. 11 (2015) 2199–2209.
[65] S.A. Tawfik, X.Y. Cui, S.P. Ringer, C. Stampf, TDDFT Study of the Optical Excitation of Nucleic Acid Bases-C60 Complexes, J. Phys. Chem. A 121 (2017) 9058–9063.
[66] S. El Arrouji, K. Karrouchi, A. Berisha, K.I. Alaoui, I. Warad, Z. Rais, S. Radi, M. Taleb, M. Ansar, A. Zarrouk, New pyrazole derivatives as effective corrosion inhibitors on steel-electrolyte interface in 1 M HCl: Electrochemical, surface morphological (SEM) and computational analysis, Colloids and Surfaces A: Physicochemical and Engineering Aspects 604 (2020) 125325–125340.
[67] I. Badran, S. Tighadouini, S. Radi, A. Zarrouk, I. Warad, Synthesis, structural, biocomputational modeling and antifungal activity of novel armed pyrazoles, J. Mol. Struct. 1229 (2021) 129799–129807.
[68] I. Warad, S. Musameh, I. Badran, N. N.Nassar, P. Brandao, C.J. Tavares, A. Barakat, Synthesis, solvatochromism and crystal structure of trans-[Cu(Et2NCH2CH2NH2)2.H2O](NO3)2 complex: Experimental with DFT combination, J. Mol. Struct. 1148 (2021) 328–338.
[69] A.M. Khedr, M. Gaber, R.M. Issa, H. Erten, Synthesis and spectral studies of 5-[3-(1,2,4-triazolyl-azo]-2,4-dihydroxybenzaldehyde (TA) and its Schiff bases with 1,3-diaminopropane (TAAP) and 1,6-diaminohexane (TAAH). Their analytical application for spectrophotometric microdetermination of cobalt(II). Application in some radiochemical studies, Dyes Pigments 67 (2005) 117–126.
[70] J. Tauc, R. Grigorovici, A. Vancu, Optical properties and electronic structure of amorphous Germanium, Phys. Status Sol. B 15 (2) (1966) 627–637.